Chapter 5

Effect of 80 MeV O^{6+} ions on Pure Polymers

Abstract

This chapter deals with the electrical, mechanical(hardness) thermal and structural characteristics of 80 MeV, O^{6+} ion irradiated PI, PC, PES and blended PVC+PET polymeric blend films at different ion fluences by different characterization techniques viz dielectric study, Vickers microhardness, FTIR spectroscopy, differential scanning calorimetry and thermogravimetric analysis.

5.0 Introduction

During irradiation, various physical and chemical processes take place in the polymer. Coulombic interaction between ions and electrons of host atoms, excessive bond stretching due to localized energy deposition, and atomic displacement by nuclear collision can release pendent atoms such as hydrogen, and cause bond breakge or chain scission. Thus, various gaseous molecular species are relased during irradiation. The most prominent speices are hydrogen, molecular scission products from the end groups as well as pendent groups of the polymer, and their reaction products. Radicals or dangling bonds are created by the release of pendent atoms such as hydrogen. Cross linking occurs when two free dangling bonds on neighbouring chain unite, where as double or triple bonds are formed if two neighbouring radicals in the same chain unite. It has been well established that mechanical, physical and chemical properties changes in polymers are determined by the magnitude of cross linking and scission and that cross linking enhances mechanical stability while scission degrades mechanical strength. Although both electronic and nuclear energy transfer can induce cross linking as well as scission as would be intuitively expected, experimental evidence suggests that electronic stopping causes more cross linking while nuclear stopping causes more scission [1].

We have studied the effect of high energy ion beam irradiation on the following polymers because of its important application in the high energy radiation field.

5.1 Polyimide (PI)

5.2 Polycarbonate (PC)

5.3 Polyether sulfone (PES)

5.4 PVC+PET Blend

we have discussed the preparation of samples, irradiation etc. and measurement by different characterization techniques in Chapter 2.

5.1 Polyimide (PI)

5.1.1 Introduction

Polyimide (PI) is one of the heat resistive and most technologically important polymers which have attracted the attention of scientists and material engineers during the last few decades. It has wide applications in different technologies especially in nuclear and satellite fabrication technology. It has sufficient ultimate tensile strength (U.T.S.) and its working temperature ranges from liquid helium temperature to 400°C for continuous use. PI represents an important class of high temperature, solvent resistant polymers. Aromatic heterocyclic polyimides are typical of most commercial polyimide. This polymer has such incredible mechanical and thermal properties so that it is used in place of metals and glass in many high performance applications in the electronics, automotive and even the aerospace industries. The properties arise from strong intermolecular forces between polymer chains. PI usually is in two forms. The first of these has a linear structure where the atoms of the imide groups are part of a linear chain. The second of these structures is a hetero cyclic structure where the imide groups are part of a cyclic unit in the polymer chain.

The effects of keV-MeV light and heavy ion irradiation have been studied extensively. Xu et al. [2] and Fink et al. [3] investigated the low and heavy ions induced chemical and structural modifications in PI films using FTIR spectroscopy. Terai and Kobayashi [4] studied the composition and structural changes of PI at different fluences of 4 MeV Ni^{3+} ions, using surface characterization technique and electrical resistance

177

measurements. Virk et al [5] studied the physical and chemical response of 70 MeV carbon ion irradiated PI film using UV-visible, FTIR, and XRD techniques. Mishra et al. [6] studied the spectroscopy and thermal behaviour of 2 MeV electron irradiated PI by using FTIR spectroscopy, TGA, and DSC measurements. Shah et al. [7] studied micro hardness and radiation damage of PI using a 3 MeV proton beam. Sharma et al. [8] studied the blister formation on the surface of PI films using 50 MeV Li^{3+} ions. In the present work, we have studied the effects of 80 MeV O^{6+} ion irradiation on the microhardness, electrical, thermal, and structural behaviors of polyimide films at different fluences [9].
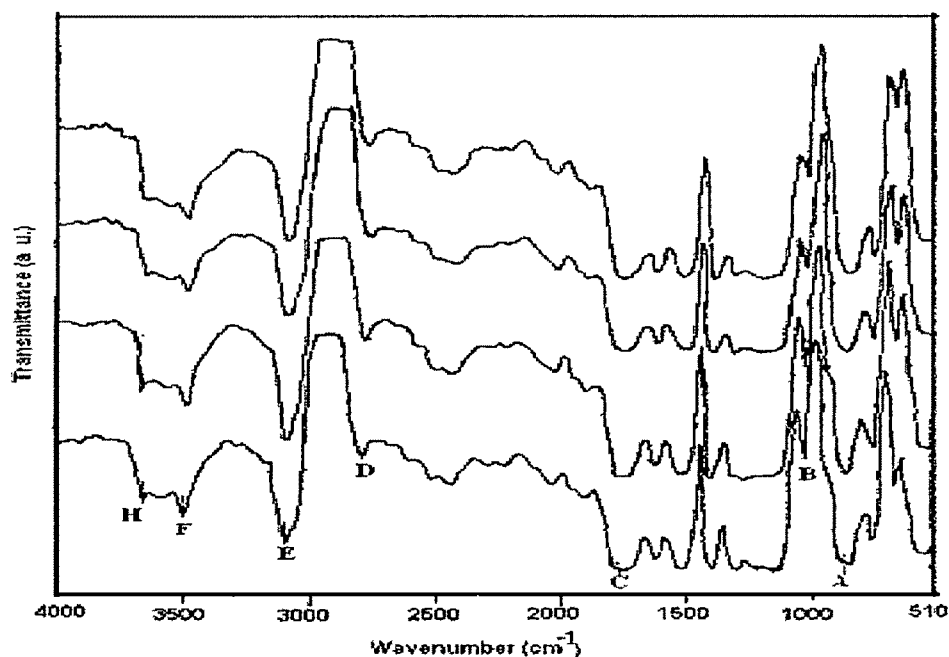
5.1.2 Result and Discussion

When a highly energetic charged ion strikes a polymeric target, it loses its energy by two mechanisms known as electronic and nuclear stopping. The electronic stopping power of the ions near the sample surface, $(dE/dx)_e$ is 6.25×10^1 eV/ Å and where as nuclear stopping power, $(dE/dx)_n$ is 3.47×10^{-2} eV/Å. The projected range of 80 MeV O^{6+} ions in polymer was calculated to be 88.2 μm using the SRIM-2003 code [10].

5.1.3 FTIR Analysis

The FTIR spectra from pristine and irradiated polyimide samples are shown in Fig 5.1. The absorption bands as obtained from the pristine spectrum are identified as (A) 932 cm^{-1}: C-C stretching vibration; (B) 1015 cm^{-1}: C-O-C stretching of ester; (C) 1730cm^{-1}: C=O stretching vibration; (D) 2777 cm^{-1}: C-H stretching vibration; (E) 3073 cm^{-1}: aromatic C-H stretching vibration; (F) 3486 cm^{-1}: C-H bending vibrations; (G) 3630 cm^{-1}: O-H stretching vibration. There was only a slight change in the signal intensity from the irradiated sample as compared to the pristine sample. This is consistent with resistance of

the polyimide sample to change by ion irradiation. The presence of ladder structure of

bonds may be responsible for such a high resistance. The minor changes in the peaks of

irradiated samples may be due to the breakage of one or two bonds in the ladder structure,

but this will not change the overall structure of the polymer. These observations confirm

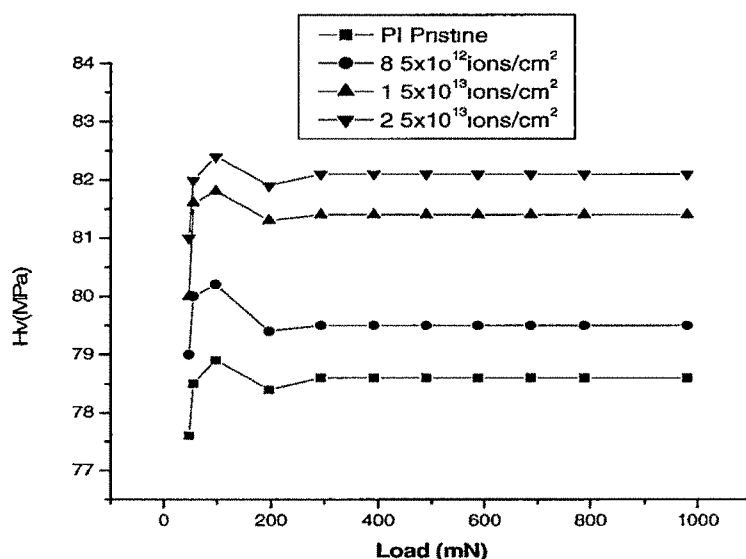that PI is resistant to bond degradation under ion irradiation [5, 8].

Figure 5.1 FTIR spectra of pristine and irradiated polyimide films.

5.1.4 Microhardness

We have stduied the microharndess by menas of Vicker's microhardness tester. The

Vicker's microhardness was calculated using equation 2.10 (article 2.4.2) as discussed in

Chapter 2.

Fig 5.2 shows the plot of the Vickers' microhardness (H_v) versus applied load (P) at different fluences. It is evident that H_v value increases with the load up to 100 mN and then saturates beyond the load of 400 mN. The increase of H_v with load can be explained on the basis of the strain hardening phenomenon. On applying the load, the polymer is subjected to some strain hardening. Beyond a certain load the polymer exhausts its strain hardening capacity and the hardness becomes constant. The rate of strain hardening is greater at low loads and decreases at higher loads [7, 8].

As it can be seen, the hardness becomes independent of the load for loads more than 400mN. The value obtained from the saturation region, therefore, represents the true hardness of the bulk material, since at high loads the indenter penetration depth is also high and surface effects become insignificant. It is also observed that the hardness increases as fluence increases. This may be attributed to the cross-linking phenomenon [11].

Legend:
- PI Pristine
- 8 5x10^{12}ions/cm^2
- 1 5x10^{13}ions/cm^2
- 2 5x10^{13}ions/cm^2

Y-axis: Hv(MPa)
X-axis: Load (mN)

Figure 5.2 Plot of hardness (H_v) versus applied load (P) for pristine and irradiated polyimide films.

5.1.5 AC Electrical Frequency Response

Electrical properties of pristine and irradiated samples were studied using an LCR meter in the frequency range 50 Hz to 10 MHz. The resistance, capacitance and dielectric loss measurements were carried out at ambient temperature. AC conductivity was calculated using equation 2 5 and dielectric constant by equation 2.8 as discussed in article 2.4.1 of Chapter 2.

5.1.5 (a) Conductivity vs frequency

Figure 5.3 shows the variation of conductivity with frequency (f in Hz) for pristine and irradiated polyimide films. A sharp increase in conductivity at around 100 kHz has been observed in pristine as well as irradiated samples. It is also observed that conductivity increases as fluence increases. The increase in conductivity due to irradiation may be attributed to scissioning of the polymer chains, resulting in an increase of the mobile radicals, unsaturation, etc. An AC field of sufficiently high frequency applied to the metal-polymer-metal structure may cause a net polarization which is out of phase with the field. This would result in increased AC conductivity; it appears at frequencies greater than that at which traps are filled or emptied [12,13].
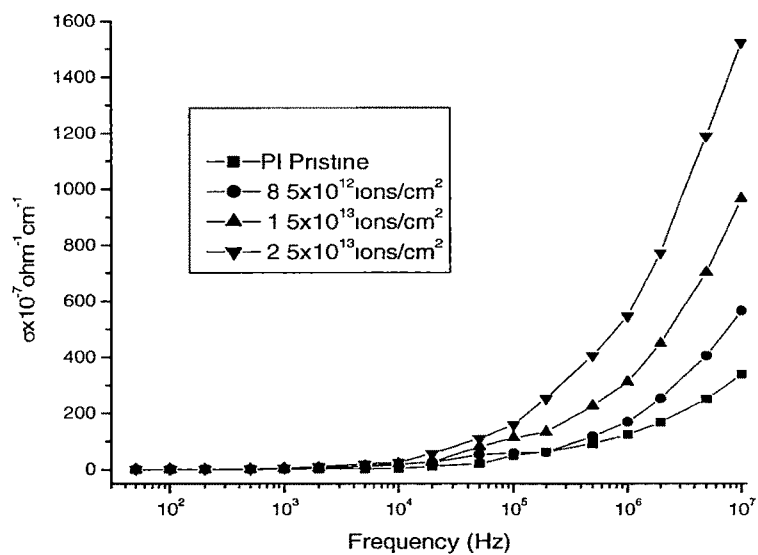
5.1.5 (b) Dielectric loss vs frequency

Figure 5.4 shows the variation of loss factor tan δ with frequency for pristine and irradiated samples. It is observed that the variation of tan δ with frequency is similar for both pristine and irradiated samples. It is also observed that tan δ increases as fluence increases. The growth tanδ as the increase in conductivity is brought about an increase in the conduction of residual current and the conduction of abdorbance current [13], tan δ has positive values indicating the dominance of inductive behavior.

181

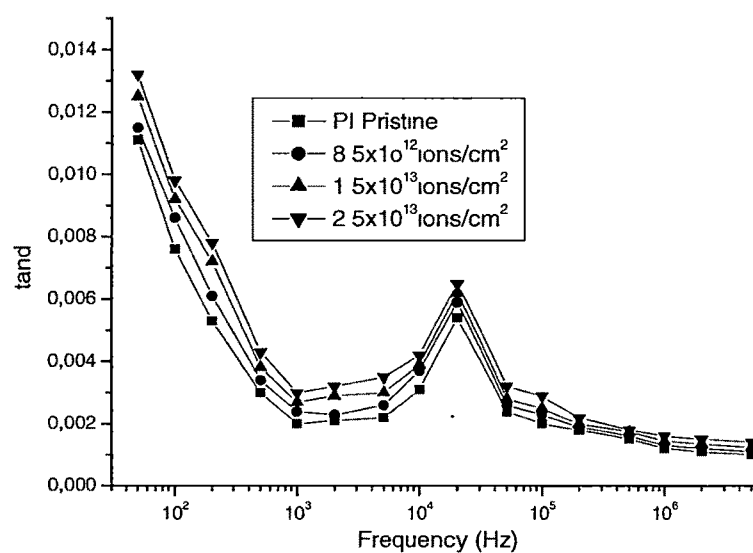## 5.1.5 (c) Dielectric constant vs frequency

Figure 5.5 shows the variation of dielectric constant with frequency for the pristine and irradiated samples. It is seen that the dielectric constant remains almost constant over a wide frequency range up to 100 kHz. At these frequencies, the mobility of the free charge carriers is constant and so the dielectric constant presumably remains unchanged. It is also observed that dielectric constant increases as fluence increases. The increase in dielectric properties due to irradiation may be attributed to scissioning of polymer bonds and as a result increase in free radicals and unsaturation etc. As frequency increases further (i.e. beyond 100 kHz), the charge carriers migrate through the dielectric and get trapped against a defect sites and induced an opposite charge in its vicinity. At these frequencies, the polarization of trapped and bound charges can not take place and hence the dielectric constant decreases [14].

The dielectric constant decreases at higher frequencies (i.e. beyond 100kHz) and obeys the Universal law [12,14] of dielectric response given by $\varepsilon \, \alpha \, f^{n-1}$, where n varies from zero to one, the value of n=0.34 for pristine; 0.32 at the fluence of 8.5×10^{12} ions/cm^2, 1.5×10^{13} ions/cm^2 and 0.31 at the fluence of 2.5×10^{13} ions/cm^2 respectively. The observed nature of the fluence dependence of dielectric constant in studied frequency range can be explained by the prevailing influence of the enhanced free carriers due to the irradiation [15].
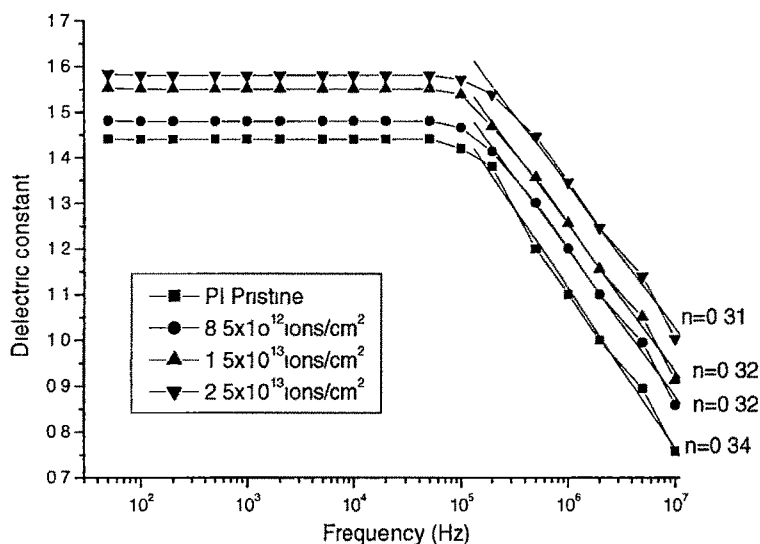
Figure 5.3 conductivity versus frequency for pristine and irradiated polyimide films.

Figure 5.4 Plot of dielectric loss versus frequency for pristine and irradiated polyimide films.

Figure 5.5 Plot of dielectric constant versus frequency for pristine and Irradiated polyimide films.

5.1.6 Thermal Analysis

(Thermogravimetric Analysis and Differential Scanning Calorimetry)

The decomposition behavior of the polymer was studied by thermogravimetric analysis as shown in Fig.5.6. In all the cases (pristine and irradiated) a stable zone (no weight loss), slow decomposition zone, fast decomposition zone and residual decomposition zone were observed. The stable zone of the pristine sample was found to extend up to $492\,^{\circ}C$. This limiting temperature became lower as a function of increased fluence and reached values of $246\,^{\circ}C$ and $135\,^{\circ}C$ for PI irradiated at a fluence of 8.5 x 10^{12} ions/ cm^2 and 2.5×10^{13} ions/cm^2 respectively. The irradiation presumably enabled the polymers to undergo a slow decomposition from the moment of application of heat.

184

This slow decomposition showed a weight loss of about 0.5%, 3.7%, and 5.2% for pristine and irradiated samples at a temperature of 400°C. Around 50% of the sample material remained undecomposed in all cases. Thermograms indicate that the composition of the sample degrades progressively during irradiation due to the emission of hydrogen gas and /or other volatile gases, which implies that chain scission proceeds preferentially compared with cross linking.

Figure 5.7 shows the DSC thermograms of pristine and irradiated samples. Heat distortion temperature was observed around 350 °C, no significant change was observed in irradiated ($2\,5\times10^{13}$ ions/cm^2) sample. As the DSC study was done in temperature range 40 °C-350 °C, no glass transition temperature (T_g) and melting temperature (T_m) were obtained.
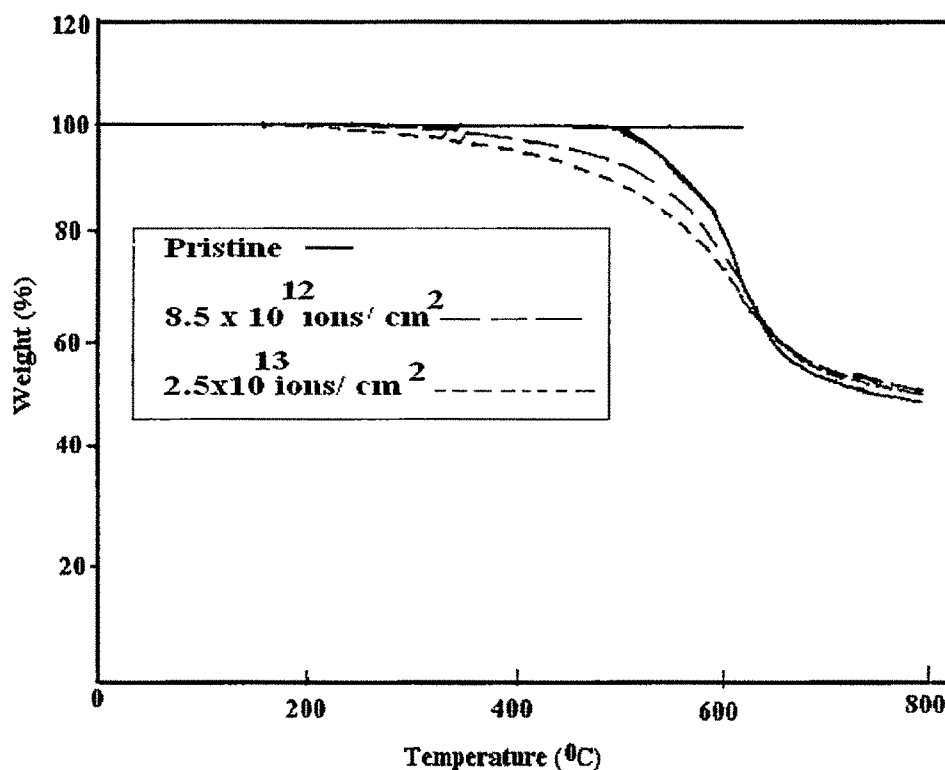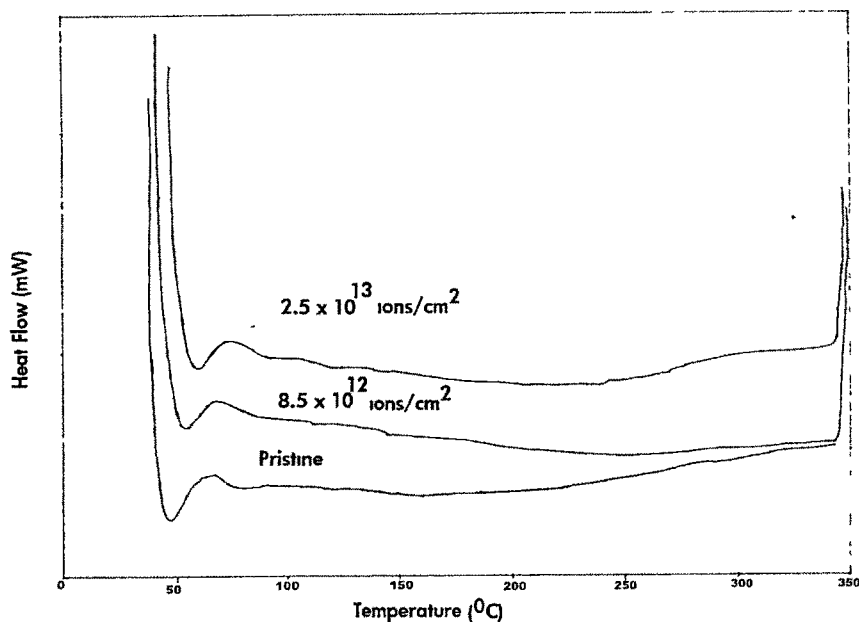

Figure 5.6 TGA thermograms of pristine and irradiated polyimide films.

Figure 5.7 DSC thermograms of pristine and irradiated PI films.

5.1.7 Conclusion

Though there was no prominent variation in the absorbance bands of PI caused by O^{6+} ion irradiation, there was a modification in the thermal properties of the polymer, which was found to be fluence dependent. The Vickers' hardness of the polymer increases as fluence increases, probably due to cross linking without any degradation effect as corroborated with FTIR spectra. The true bulk hardness of the film was obtained at load greater than 400 mN. A sharp increase in AC electrical conductivity was observed around 100 kHz frequency and conductivity increased as fluence increased. The dielectric constant and loss factor were observed to change significantly with the fluence. This may be due to scissioning of polymeric chains. It is also observed that it obeys Universal law of dielectric response at high frequency.

5.2 Polycarbonate (PC)

5.2.1 Introduction

Polycarbonate (makrofol-DE) is an amorphous engineering thermoplastic notable for its high impact resistance. It has reasonably good temperature resistance, good dimensional stability and low creep but some what limited chemical resistance and is prone to environmental stress cracking. It is widely used today to prepare track-etched membranes. PC particle track etched membranes are used as templates in nano-tubes and nano wires manufacturing [16].

There are numerous reports on PC using energetic ions, but mechanical (hardness) and electrical properties induced by swift heavy ion (SHI) irradiation did not receive much attention. Ferain and Legras [17] studied the chemical modifications induced by SHI irradiations (Ar ion 4.5 MeV/amu) in a model compound of PC, ie diphenyl carbonate. Steckenreiter et al [18] studied the degradation processes in PC induced by SHI irradiations with electronic stopping power $(dE/dx)_e$ higher than 4.0 MeV mg^{-1} cm^2. They have reported the alkyne formation in all irradiated polymer using insitu FTIR spectroscopy. Chipara et al [19] reported electron spin resonance investigations of SHI irradiated PC. They have discussed the nature of free radicals as well as exchange interactions among them on the basis of track structure. Zhu et al [20] and Wang et al [21] investigated chemical changes in PC induced by very high energetic ions (>GeV) using ex-situ FTIR spectroscopy. They also reported alkyne formation in irradiated PC with electronic stopping power $(dE/dx)_e$ values higher than 3.5 MeV mg^{-1} cm^2. Dehaye et al. [22] investigated the chemical modification induced in bisphenol A polycarbonate by SHI using in situ FTIR spectroscopy. They observed new vibrational bonds in the

irradiated samples Studies on thermal and structural properties of 62 MeV protons irradiated PC were carried out by Mishra et al [23] at different doses and it was reported that thermal stability decreases as dose increases. The aim of the present work is to investigate the radiation induced changes in electrical, mechanical, thermal and structural properties of 80MeV O^{6+} ions irradiated polycarbonate (makrofol-DE) at different fluences [24].

5.2.2 Result and Discussion

When an energetic charged ion strikes a polymeric target, it loses its energy by two mechanisms known as electronic and nuclear stopping. The electronic stopping power of the beam $(dE/dx)_e$ is 5.528×10^1 eV/ Å and nuclear stopping power of the beam $(dE/dx)_n$ is 3.148×10^{-2} eV/Å. The projected range of 80 MeV O^{6+} ions in polymer was calculated to be 98.2µm using SRIM-2003 code [10]. The thickness of the polymer is 4 times larger than the projected range of the ions in the polymer. Hence, the beam was stopped in the polymer and maximum dissipation of heat took place at the end.

5.2.3 FTIR Analysis

The FTIR spectra of pristine and irradiated PC films are shown in Figure 5.8. The absorption bands as obtained from the pristine spectrum are identified as (A) 765 cm⁻¹:out of phase skeletal vibration of C-H deformation; (B) 1030 cm⁻¹:C-O stretching vibration; (C) 1645cm⁻¹: C=C phenyl ring stretching vibration; (D) 1770 cm⁻¹: C=O stretching vibration; (E) 2484 cm⁻¹: hydroxyl stretching bond; (F) 2928 cm⁻¹:CH₃ stretching vibrations; (G) 3080 cm⁻¹: C-H stretching vibration of aromatic compounds. It is observed that there is no change in overall structure of the polymer but minor changes in intensities were observed. The minor changes in the peak- intensities of irradiated

samples may be due to the breakage of few bonds in the ladder but this will not change
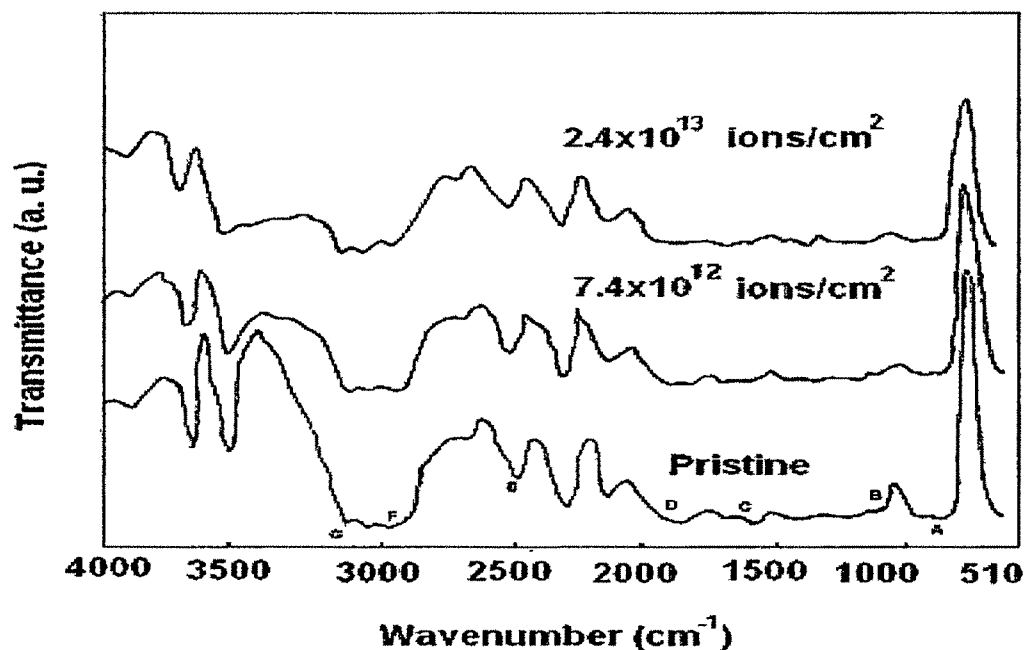
the overall structure of the polymer [24].

Figure 5.8 FTIR spectra of pristine and irradiated PC films.

5.2.4 Microhardness

The Vickers' hardness value (H_v) was determined with microhardness tester with a

Vickers' diamond pyramidal indenter of a Carl Zeiss optical microscope. The indentation

diagonals were measured to using a micrometer eyepiece. The microhardness was

calculated using equation 2.10 as discussed in article 2.4.2 of Chapter 2.

The load dependence hardness was measured in the load range 50-1000 mN for a constant

loading time of 30 seconds. Figure 5.9 shows the plot of the Vickers' microhardness (H_v)

versus applied load (P) at different fluences It is evident that H_v value increases with the load up to 300mN and then decreases and then saturates beyond the load of 400 mN. The value obtained from the saturation region, therefore, represents the true hardness of the bulk material, since at high loads the indenter penetration depth is also high and surface effects become insignificant. It is also observed that the hardness increases as fluence increases, which can presumably be due to the cross-linking of some of the degraded molecules by irradiation [11].

5.2.5 AC Electrical Frequency Response

AC Electrical properties of pristine and irradiated samples were studied using an LCR meter in the frequency range 50 Hz to 10 MHz. The resistance, capacitance and dielectric loss measurements were carried out at ambient temperature AC conductivity was calculated using equation 2.5 and dielectric constant by equation 2.8 as discussed in article 2.4.1 of Chapter 2.

5.2.5 (a) Conductivity vs frequency

Figure 5.10 shows the variation of conductivity with frequency (f in Hz) for pristine and irradiated polycarbonate films. A sharp increase in conductivity at around 100 kHz has been observed in pristine as well as irradiated samples. It is also observed that conductivity increases as fluence increases. The increase in conductivity due to irradiation may be attributed to scissioning of the polymer chains and resulting in an increase of the free radicals, unsaturation, etc. An AC field of sufficiently high frequency applied to metal-polymer-metal structure may cause a net polarization, which is out of the phase with the field. This results in AC conductivity, it appears at frequency greater than that at which traps are filled or emptied [12-14].

5.2.5 (b) Dielectric loss vs frequency

Figure 5.11 shows variation of tan δ with frequency for pristine and irradiated samples. It reveals that tanδ drop shraply as frequency increases and become constant beyond a frequency of 1 kHz. This indicates tht loss factor depends on frequency below 1 kHz and became constant beyond this frequency, suggesting that PC films can be used as · dielectric in capacitor, above 1 kHz frequency. It is observed that loss factor increases moderately as fluence increases. The growth in tanδ as the increase in conductivity is brought about by an increase in the conduction of residual current and the conduction of absorbance current [13].

5.2.5 (c) Dielectric constant vs frequency

Figure 5.12 shows the variation of dielectric constant with frequency for the pristine and irradiated samples. It is seen that the dielectric constant remains almost constant over a wide frequency range upto 100 kHz At these frequencies, the mobility of free charge carriers is constant and so dielectric constant remains unchanged. It is also observed that dielectric constant increases as fluence increases. The increase in dielectric properties due to irradiation may be attributed to scissioning of polymer bonds and as a result increase in free radicals and unsaturation etc. The dielectric constant decreases at higher frequencies (i.e. beyond 100kHz) and obeys the Universal law [12-14] of dielectric response given by $\varepsilon \, \alpha \, f^{n-1}$, where n varies from zero to one, the value of n=0.76 for pristine and 0.69, 0.63 and 0.56 for irradiated samples at the fluence of 7.4×10^{12} ions/cm^2, 1.2×10^{13} and 2.4×10^{13} ions/cm^2 respectively. The observed nature of the fluence dependence of dielectric constant in studied frequency range can be explained by the prevailing influence of the enhanced free carriers due to the irradiation [15].
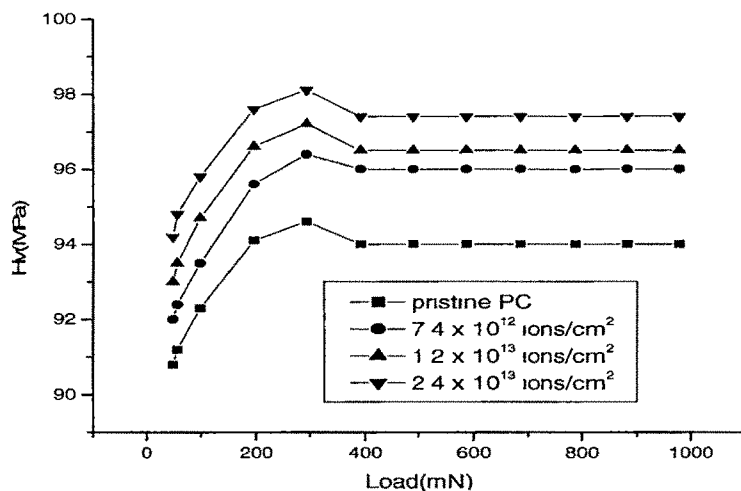
191

Figure 5.9 Plot of hardness (H_v) versus applied load (P) for pristine and irradiated PC films.

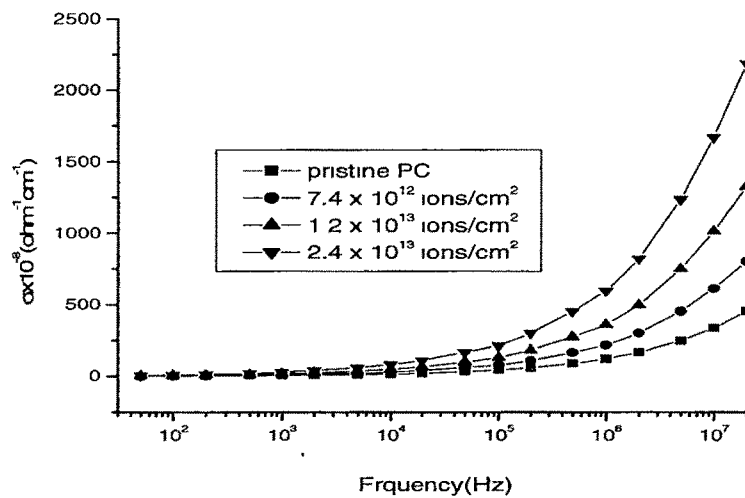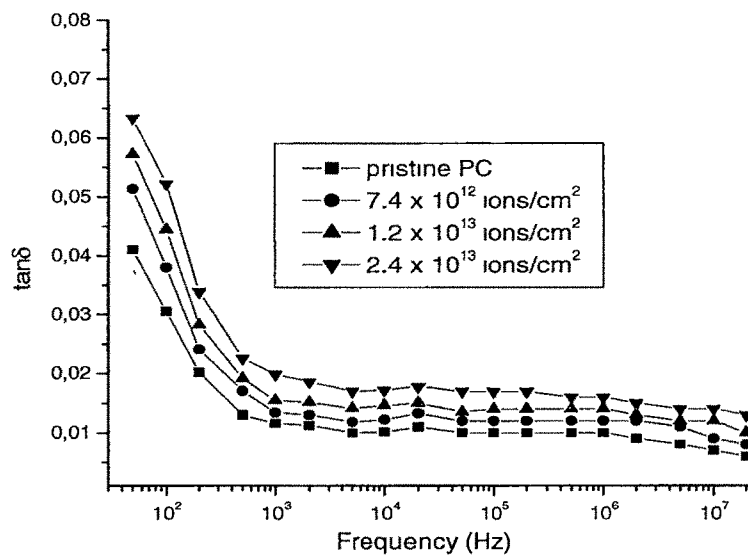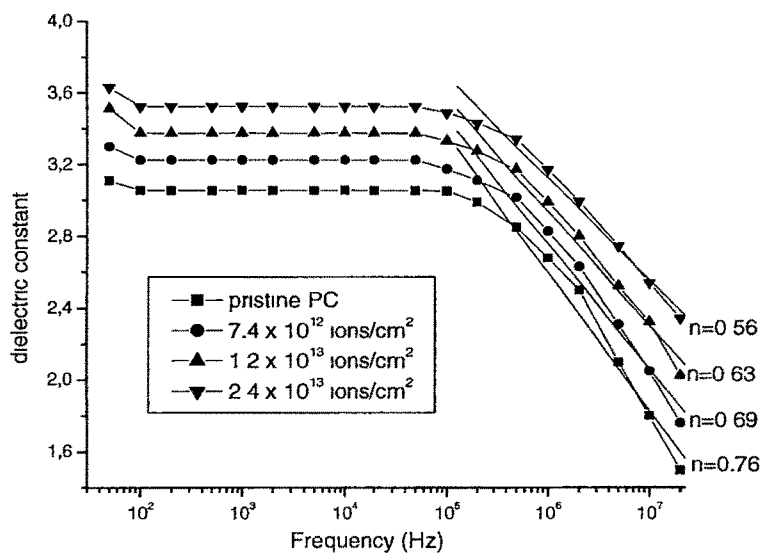**Fig 5.10** AC conductivity versus frequency for pristine and irradiated PC films.

Figure 5.11 Variation of tan δ with frequency for pristine and irradiated PC films.

Fig 5.12 Plot of dielectric constant versus frequency for pristine and irradiated PC films.

5.2.6 Thermal Analysis

(Thermogravimetric Analysis and Differential Scanning Calorimetry)

The decomposition behavior of the polymer was studied by thermogravimetric analysis as shown in Figure 5.13. In all the cases (pristine and irradiated) a stable zone (no weight loss), slow decomposition zone, fast decomposition zone and residual decomposition zone were observed. The stable zone of the pristine was found up to 435 °C, where as the stable zone of irradiated sample at the fluence of 2.4×10^{13} ions/cm^2 reduced slightly to 418 °C. There is no significant change in the stability of irradiated polymer at the fluence of 2.4×10^{13} ions/cm^2.
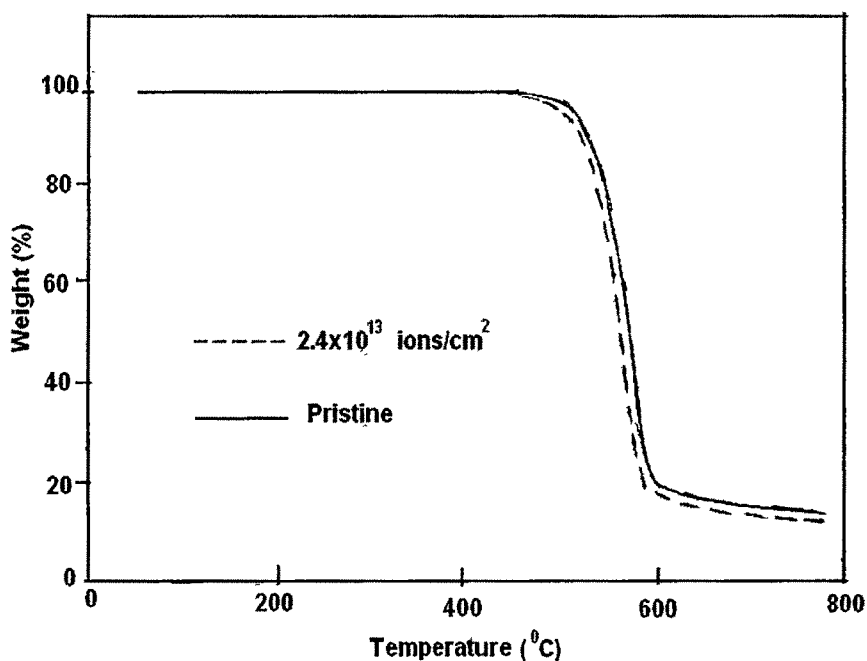

Figure 5.13 TGA thermograms of pristine and irradiated PC films.

Figure 5 14 shows the DSC thermograms of pristine and irradiated samples. The glass transition temperature was observed around 147 °C for pristine sample and no significant change was observed in irradiated samples It reveals that PC is thermally stable upto the above fluence used. The minor change in stability has been observed due to breakage of few bonds in polymer structure.
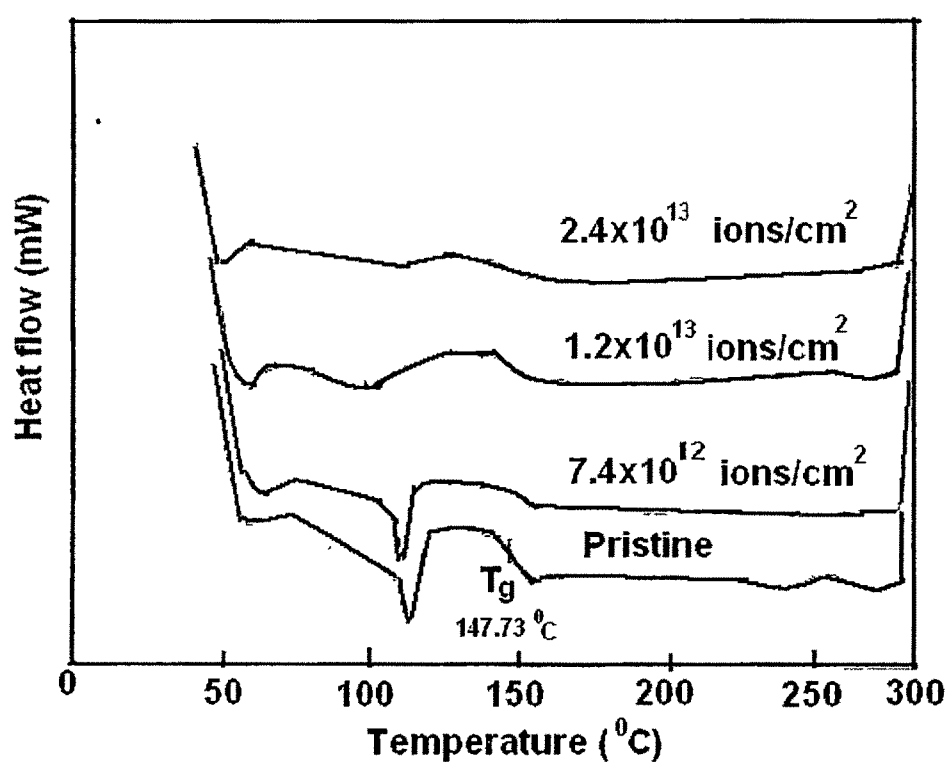

Figure 5.14 DSC thermograms of pristine and irradiated PC films.

195

5.2.7 Conclusion

There was no significant variation in the absorbance bands and thermal stability of PC due to 80 MeV O^{6+} ions irradiation at the fluence of 2.4×10^{13} ions /cm^2. Hence, PC is radiation resistance up to the above fluence. The Vickers' hardness of the polymer increases as fluence increases, which can presumably by due to the cross linking of some of the degraded molecules by irradiation. The true bulk hardness of the film was obtained at loads greater than 400 mN A sharp increase in conductivity has been observed around 100 kHz frequency and conductivity increases as fluence increases. The dielectric constant and loss factor are observed to change significantly with the fluence. This might be attributed to breakage of chemical bonds and which results in the increase of free radicals, unsaturation etc. It is also observed that it obeys Universal law of dielectric response at high frequency.

5.3 Polyether sulfone (PES)

5.3.1 Introduction

Ion irradiation is a convenient method for altering the properties (mechanical, electrical, thermal etc.) of polymers and these changes are related to the changes in the chemical structures of the polymers [25] The effects of irradiation with polymer results in the formation of gaseous products accompanied by cross-linking (ie formation of intermolecular bonds), degradation (i.e. the scission of bonds in the main polymer chain and in side chains) and some other secondary processes These transformations and their radiation chemical yields have been investigated and calculated for many polymers [26]. Information about yields and composition of gases produced by polymer irradiation in combination with data concerning irradiated polymers (changes in molecular weight, different spectral characteristics etc) is useful to explain the mechanisms and efficiency of radiation chemical transformations in these materials. It should be stressed that the evaluation of polymers radiation stability (resistance to irradiation) is of great importance in nuclear reactors, radio isotopes installation, electron and other particles accelerators or in device operating under outer space conditions. The absorption of radiation energy in sufficient amounts will effect the number of charge carriers in an insulating materials to an extent determined by its molecular structure and chemical composition. The dielectric response of materials provides information about the orientational and translational adjustment of mobile charges present in the dielectric medium in response to an applied electric field. The most important property of the dielectric material is its ability to be polarized under the action of the field. The outstanding properties of aromatic polymer (PES), such as thermo- oxidative stability and superior chemical resistance lead the use of

this polymer in high temperature environment PES is used in micro-electronics, aerospace, and medical application etc.

There are few reports on this polymer using energetic low and high ion beams. Bridwell et al. [27] studied the dose rate effects on the electrical properties of several polymers (PES, PEEK, PS, PAN and PSA) implanted by 50 keV atomic and molecular nitrogen ions. They have also reported that the electrical conductivity of these polymers shows significant changes with varying dose rate. They have reported that aliphatic or partially aliphatic polymers such as PET and PAN will reach lower resistivity than polymers that have more fully aromatic structures such as PEEK and PES. Evelyn et al. [28] irradiated stacks of thin films of PES, PS and PVC by 5 MeV helium ions and studied the radiation induced changes in chemical structure of the polymers. They observed a complex reorganization of the chemical structure. It was also reported that the disorder increases in the deeper irradiated layers of the polymer films due to the nuclear stopping power. Recently, Kumar et al. [29] studied the optical, chemical and structural modification of PES using 70 MeV carbon ion beam.

The focus of present study is to investigate the effects of 80 MeV O^{6+} ions irradiation on its electrical, mechanical, thermal and structural properties at different fluences [30].

5.3.2 Results and Discussion

When an energetic charged ion strikes a polymeric target, it loses its energy by two mechanisms known as electronic and nuclear stopping The electronic stopping power of the beam $(dE/dx)_e$ is 5.528×10^1 eV/ Å and nuclear stopping power of the beam $(dE/dx)_n$ is 3.148×10^{-2} eV/Å. The projected range of 80 MeV O^{6+} ions in polymer was calculated to be 98.2μm using SRIM-2003 code [10].
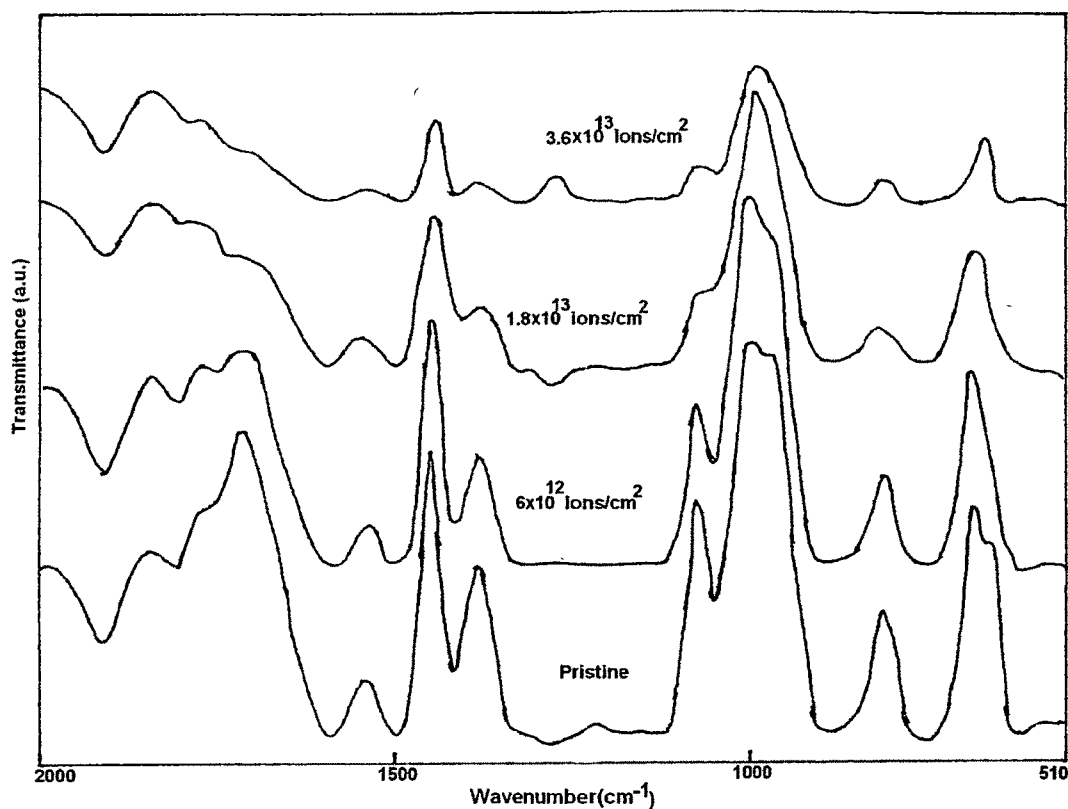
5.3.3 FTIR Analysis

The FTIR spectra of pristine and irradiated samples are shown in Fig.5.15 The absorption bands as obtained from the pristine spectrum are identified as: The absorption bands for CH_2 bonds appear in the 1410-1370 cm^{-1} and 700-720 cm^{-1} region; C-H bending vibration in the region 900-860 cm^{-1} ; -C=C stretching vibration of benzene ring occurs in the region 1620-1440 cm^{-1} and –C=C- stretching vibration at 1620 cm^{-1} ;The absorption bands corresponding to the C-O stretching vibration at 1110 cm^{-1} and sulfone stretching vibration at 1050 cm^{-1} ;Overtones and combination bonds due to C-H out of plane deformations occur in the region 2000-1660 cm^{-1} [29]. It is observed that there is a chemical degradation of the irradiated polymer by swift heavy ion irradiation and intensity of most of the functional group declines as fluence increases. The change in the intensities of the functional groups of irradiated samples may be due to breakage of bonds in the structure and creation of double/triple bonds. It is also revealed that the position of functional groups shifted to lower wave number region on increasing the fluence.
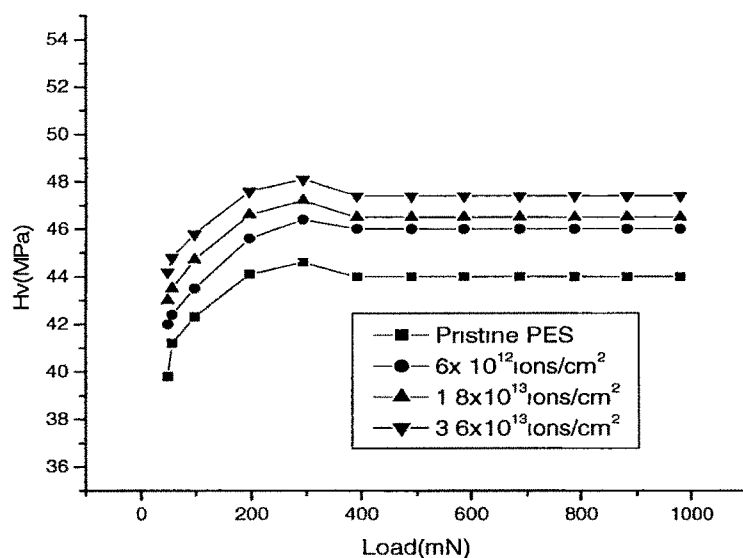
5.3.4 Microhardness

The Vickers' hardness value (H_v) was determined with microhardness tester with a Vickers' diamond pyramidal indenter of a Carl Zeiss optical microscope. The indentation diagonals were measured using a micrometer eyepiece. The microhardness was calculated using equation 2.10 as discussed in article 2.4.2 of Chapter 2.

The load dependence hardness was measured in the load range 50-1000 mN for a constant loading time of 30 s. Fig. 5.16 shows the plot of the Vickers' microhardness (H_v) versus applied load (P) at different fluences. It is evident that H_v value increases with the

load up to 300mN and then saturates beyond the load of 400mN. The value obtained from the saturation region, therefore, represents the true hardness of the bulk material, since at high loads the indenter penetration depth is also high and surface effects become insignificant. It is also observed that the hardness increases as fluence increases, which can presumably be due to the cross-linking of some of the degraded molecules by irradiation, i. e. the formation of hydrogen depleted carbon network which make polymer harder [11].

Figure 5.15 FTIR spectra of pristine and irradiated PES samples.

Hv(MPa)

54
52
50
48
46
44
42
40
38
36

—■— Pristine PES
—●— 6x 10^{12}ions/cm^2
—▲— 1 8x10^{13}ions/cm^2
—▼— 3 6x10^{13}ions/cm^2

0   200   400   600   800   1000

Load(mN)

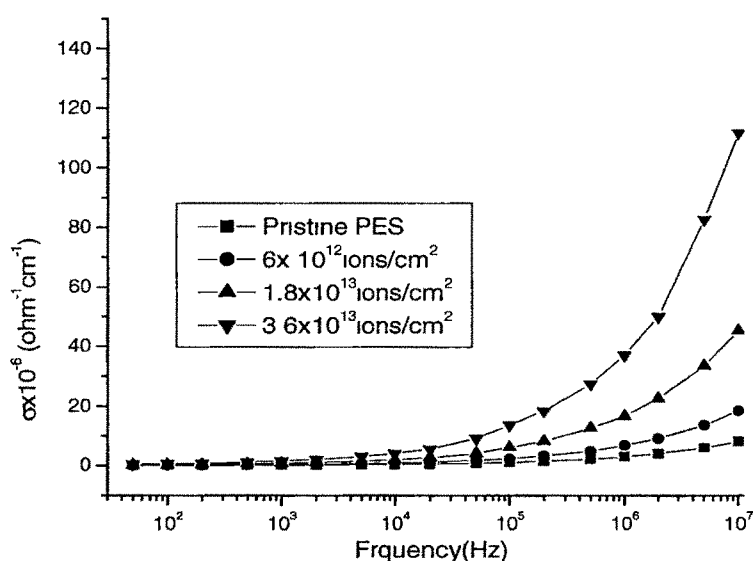**Figure 5.16 Hardness (H$_v$) versus applied load (P) for pristine and irradiated PES samples.**

5.3.5 AC Electrical Frequency Response

AC Electrical properties of pristine and irradiated samples were studied using an LCR meter in the frequency range 50 Hz to 10 MHz. The resistance, capacitance and dielectric loss measurements were carried out at ambient temperature. AC conductivity was calculated using equation 2.5 and dielectric constant by equation 2 8 as discussed in article 2.4.1 of Chapter 2.

5.3.5 (a) Conductivity vs frequency

Fig. 5.17(a) shows the variation of conductivity with frequency (f in Hz) for pristine and irradiated films. A sharp increase in conductivity has been observed in pristine as well as irradiated samples. It is also observed that conductivity increases as

fluence increases. The increase in conductivity due to irradiation may be attributed to scissioning of the polymer chains and resulting in an increase of the free radicals, unsaturation, etc. An AC field of sufficiently high frequency applied to the metal-polymer-metal structure may cause a net polarization, which is out of the phase with the field. This results in AC conductivity, it appears at frequencies greater than that at which traps are filled or emptied [12-14].
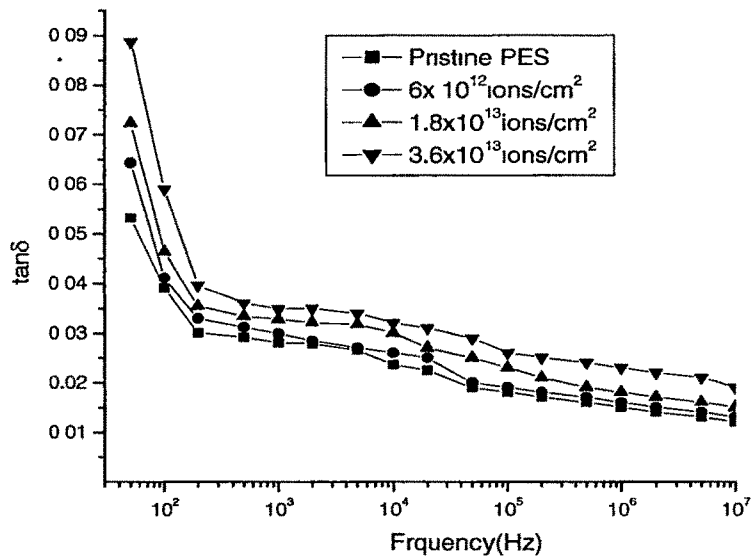

Figure 5.17(a) AC conductivity versus frequency for pristine and irradiated PES samples.

5.3.5 (b) Dielectric loss vs frequency

Fig. 517(b) shows variation of dielectric loss (tan δ) with log frequency for pristine and irradiated samples. It is observed that tan δ decreases exponentially as frequency increases. It is also observed that dielectric loss (tan δ) increases as fluence

increases. The increase in dielectric loss with fluence may be due to the scissioning of polymer chain and as a result increase in free radicals etc.
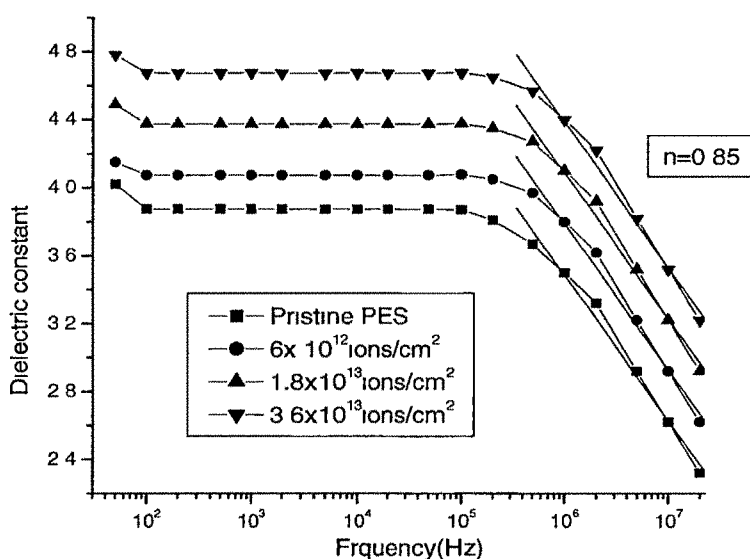

Figure 5.17 (b) Dielectric loss versus frequency for pristine and irradiated samples.

5.3.5 (c) Dielectric constant vs frequency

Fig. 5.17(c) shows the variation of dielectric constant with frequency for the pristine and irradiated samples. It is seen that the dielectric constant remains almost constant over a wide frequency range of 100 kHz and then decreases at higher frequencies. At lower frequencies, the mobility of the free charge carriers is constant and so dielectric constant remains unchanged. As frequencies increases further (i.e. beyond 100 kHz), the charge carriers migrate through the dielectric and get trapped against a defect sites and induced an opposite charge in its vicinity. At these frequencies, the polarization of trapped and bound charges can not take place and hence the dielectric constant decreases [14]. It is also observed that dielectric constant increases as fluence

increases. The increase in dielectric properties due to irradiation may be attributed to scissioning of polymer chains and as a result increase in free radicals and unsaturation etc. The dielectric constant decreases at higher frequencies (i e. beyond 100kHz) obeys the Universal law [12] of dielectric response given by $\varepsilon \alpha f^{n-1}$, with n=0.85 where n is constant for pristine and irradiated samples. The observed nature of the fluence dependence of dielectric constant in studied frequency range can be explained by the prevailing influence of the enhanced free carriers due to oxygen irradiation [15].

Figure 5.17 (c) Dielectric constant versus frequency for pristine and irradiate PES samples.

5.3.6 Thermal Analysis

(Thermogravimetric Analysis and Differential Scanning Calorimetry)

TGA thermograms of pristine and irradiated samples are shown in Fig 5.18. As depicted in figure, the stable zone for pristine and irradiated samples at the fluence of 6x

10^{12} and 1.8×10^{13} ions/cm^2 are up to the temperature of 444°C, 436°C and 408°C

respectively, though at the fluence of 3.6×10^{13} ions/cm^2, the stable zone is present only

up to 284°C. The change clearly indicates that stable zone decreases as fluence increases.

The weight loss(%) of 1.6, 2.8, 6.4 and 23.6 % has been observed for the pristine and

irradiated samples at the fluence of 6×10^{12}, 1.8×10^{13} and 3.6×10^{13} ions/cm^2 respectively at

the temperature of 500 °C. However, at the temperature of 800°C, the weight loss of

about 33% has been observed for pristine where as irradiated samples show a weight loss

of about 42-45%. After the start of degradation, the rate of degradation of pristine sample

is higher than the irradiated ones. From the data, it is evident that significant change has

been observed at the fluence of 3.6×10^{13} ions/cm^2, which is also revealed by FTIR spectra

(Fig 5.15). The activation energy for the polymer decomposition process was calculated

from the TGA patterns using the equation [31]

$\ln[\ln(m_0/m)] = - E_a/R[1/T] + \text{constant}$

Where E_a is the activation energy of decomposition, m_0 is the initial mass, m is the mass

at temperature T and R is the universal gas constant.

It is observed that activation energy (Fig.5.19) decreases from 108.03 KJ/mole to

44.24 KJ/mole for pristine and irradiated (3.6×10^{13} ions/cm^2) samples. This indicates that

irradiated sample decomposed earlier than pristine.

Fig 5.20 shows the DSC curves for pristine and irradiated PES films at the fluence

of 1.8×10^{13} and 3.6×10^{13} ions/cm^2. The glass transition temperature (T_g) was observed at

223°C in pristine and slight changes were observed in irradiated samples (ie. 220 °C at a

fluence of 3.6×10^{13} ions/cm^2). As DSC study was done in between 40°C - 300°C, no
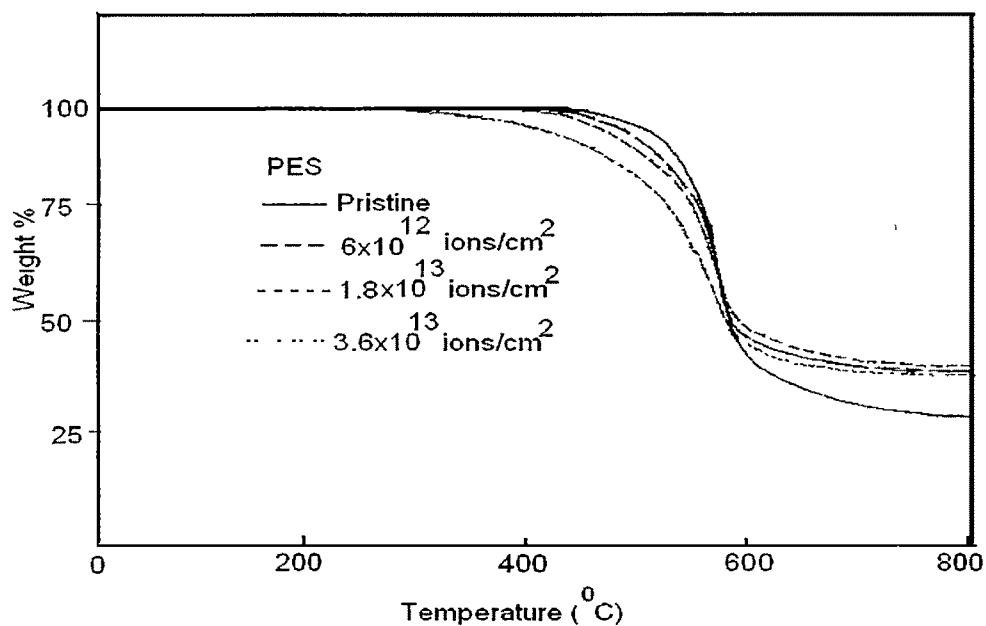
melting temperature (T_m) was observed.

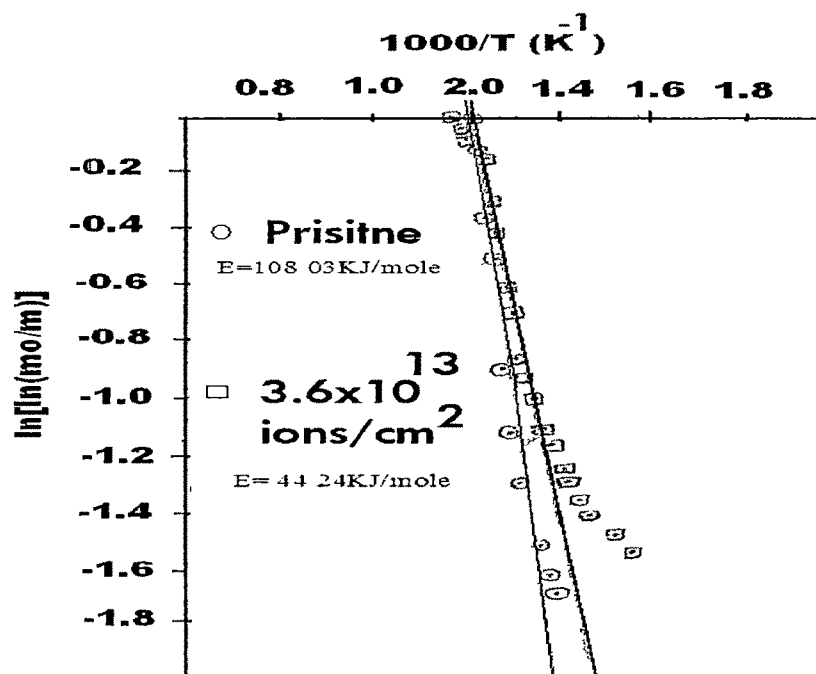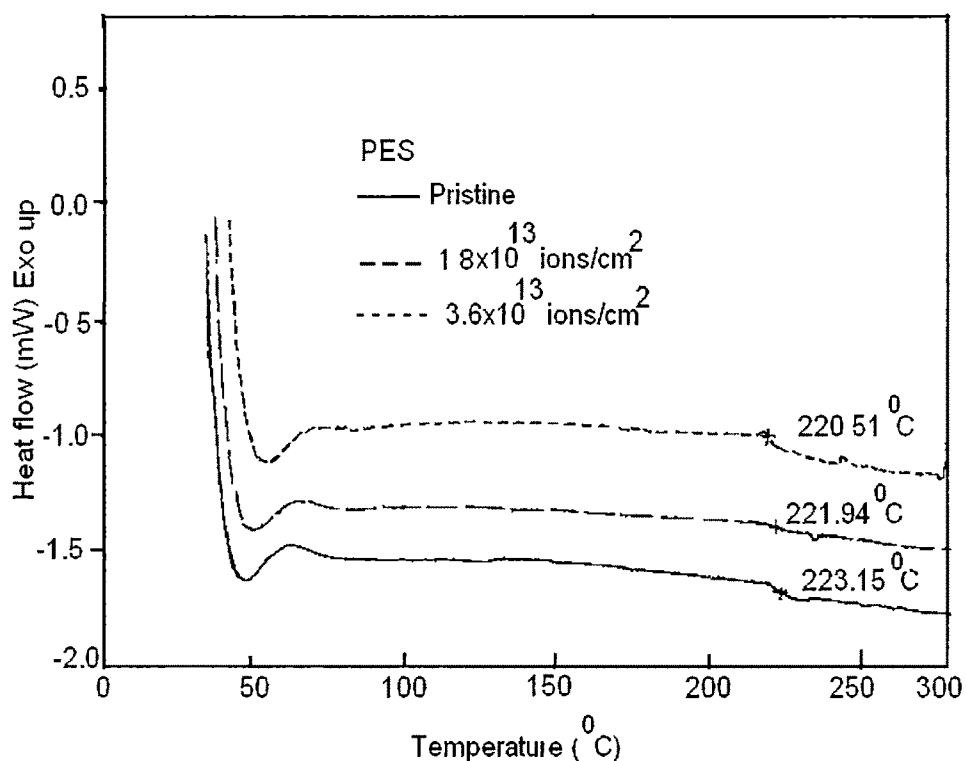**Figure 5.18 TGA thermograms of pristine and irradiated PES samples.**

Figure 5.19 ln [ln(m₀/m)] versus 1000/T (K⁻¹)for the pristine and irradiated PES samples.

Figure 5.20 DSC thermograms of pristine and irradiated PES samples.

5.3.8 Conclusion

The FTIR analysis revealed a complex reorganization of the chemical structure of the irradiated polymer and intensity of the functional groups declined as fluence increases. The Vickers' hardness of the polymer increases as fluence increases, which can presumably be due to the cross linking of some of the degraded molecules by irradiation i. e. formation of hydrogen depleted carbon network. The true bulk hardness of the film was obtained at loads greater than 400 mN. The AC electrical studies indicate that the conductivity increases on increasing the frequency and also with the fluence. Dielectric loss and constant are observed to change significantly with the fluence. This might be

attributed to breakage of chemical bonds and resulting in the increase of free radicals, unsaturation etc. It is also observed that it obeys Universal law of dielectric response.

TGA thermograms indicate that thermal stability of PES decreases as fluence increases which is also corroborated with FTIR spectra. The calorimetric measurement of 80 MeV oxygen ions irradiated PES shows very slight change in glass transition temperature (T_g). The minor change in Tg, decrease in thermal stability and intensities of functional groups of irradiated samples may be due to the breakage of few bonds in the structure of the polymer. From these observations, it may be concluded that PES is resistant to radiation degradation, since no significant changes were observed upto the fluence of 10^{13} ions/cm^2.

5.4 PVC+PET Blend Polymer

5.4.1 Introduction

In the last decades great attention has been paid to the development of polymeric blends [32,33]. The significant advantages of polymer blends are that the properties of the finished product can be tailored to the requirements of the applications, which can not be achieved alone by one polymer. The polymers with different properties and structures are usually mixed together to get polymer blends, which have different behavior. The addition of an amorphous polymer (PVC) to a crystallizable polymer (PET) can have a significant effect on miscibility, plasticization and crystallization behavior of such polymer blends. PVC has very good electrical properties where as PET was chosen because of its very good mechanical strength due to the presence of aromatic ring in the polymer structure. There has been a growing inerest towards the modification of material properties by using swift heavy ion (SHI) irradiation technique [29]. The electronic and the nuclear stopping power profile for MeV ions for polymer material show that electronic stopping power dominates at shallower penetration depth compared with nuclear stopping power which is maximum at the end of the ion track. Each stopping power induces different effects in the material due to the particular mechanisms and quantities of energy deposited [24,28].

The primary phenomenon associated with ion beam and polymer interactions are cross linking, chain scission, and emission of atoms, molecules and molecular fragments. Accordingly, the ion beam irradiation in turn influence the thermal, mechanical, electrical and other properties of the polymers that open the way to design a variety of devices with required parameters.

209

In the present study, the effect of oxygen ion irradiation on electrical, mechanical (hardness), structural and thermal properties of polymer blends of PVC and PET has been discussed at different fluences [35].

5.4.2 Results and Discussion

The projected range of 80 MeV O^{6+} ions in the polymer blend was calculated to be 92 μm using SRIM-2003 [10]. The thickness of the sample is 5 times more than the projected range. The electronic stopping power $(dE/dx)_e$ and nuclear stopping power $(dE/dx)_n$ were found to be $6.02 \times 10^{+1}$ eV/Å and 3.42×10^{-2} eV/Å respectively.

5.4.3 FTIR Analysis

The FTIR spectra of pristine and irradiated samples are shown in Fig 5 21.The absorption bands as obtained from the pristine spectrum are identified as. (A) 600-800 cm^{-1} : C-Cl stretching vibration, (B) 1015 cm^{-1} · C-O-C stretching of ester, (C) 1520 cm^{-1} : C-C stretching of phenyl group; (D) 1730 cm^{-1}: C=O stretching vibration; (E) 2800-3000 cm^{-1} : C-H stretching of CH_2 group; (F) 3258 cm^{-1}: C-H stretching vibration of the vinyl group; (G) 3000-3600 cm^{-1} : OH stretching vibration.

It is found that the aborption bands characteristic of all previously mentioned functional groups declines, conforming their detruction by irradiation and they vanish gradually as irradiation proceeds. This might be attributed to breakge of chemical bonds and formation/emission of low molecule gases and radicals.
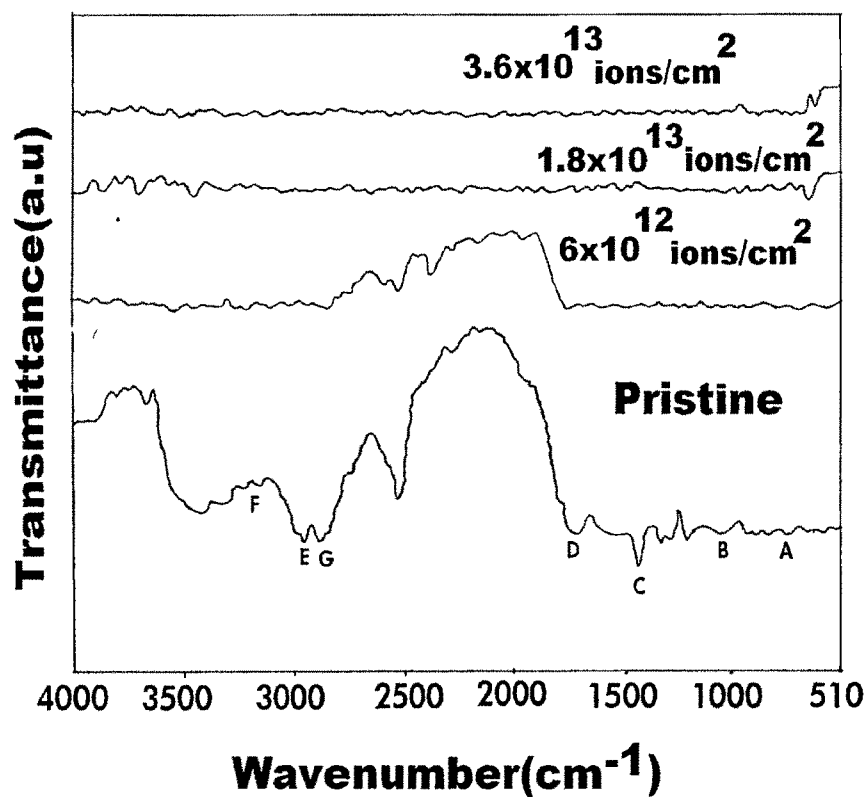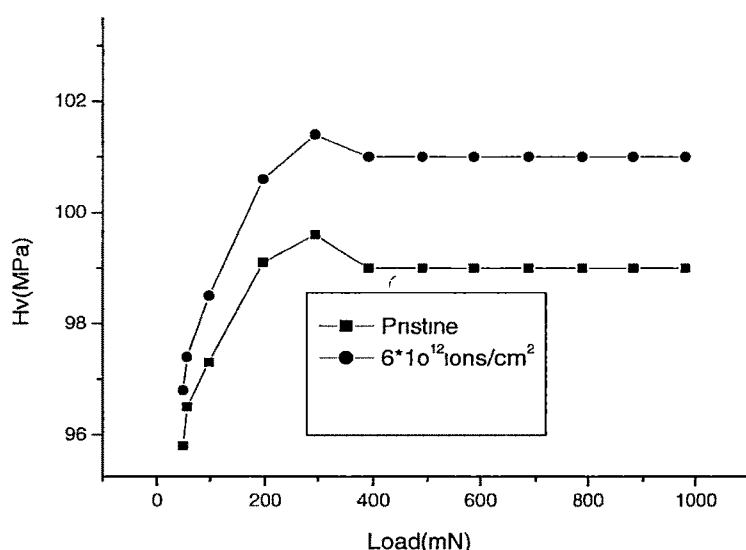
Figure 5.21 The FTIR spectra of pristine and irradiated blend samples.

5.4.4 Microhardness

The Vickers' hardness value (H_v) was determined with microhardness tester with a Vickers' diamond pyramidal indenter of a Carl Zeiss optical microscope. The indentation diagonals were measured using a micrometer eyepiece. The load dependence hardness was measured in the load range 50-1000 mN for a constant loading time of 30 s. The microhardness was calculated using equation 2.10 as discussed in article 2.4.2 of Chapter 2. Fig.5.22 shows the plot of the Vickers' microhardness (H_v) versus applied load (P) for pristine and irradiated samples. It is evident that H_v value increases with the load up to 300mN and then saturates beyond the load of 400 mN. The value obtained

211

from the saturation region, therefore, represents the true hardness of the bulk material, since at high loads the indenter penetration depth is also high and surface effects become insignificant. It is also observed that the hardness increases as fluence increases, which can presumably be due to the cross-linking of some of the degraded molecules by irradiation, i.e. the formation of hydrogen depleted carbon network which make polymer harder [11]. At higher fluences i.e. 1.8×10^{13} ions/cm^2 and 3.6×10^{13} ions/cm^2, samples became dark brown and it was not possible to see the indentation.

Figure 5.22 Hardness (H_v) versus applied load (P) for pristine and irradiated samples.

5.4.5 AC Electrical Frequency Response

AC Electrical properties of pristine and irradiated samples were studied using an LCR meter in the frequency range 50 Hz to 10 MHz. The resistance, capacitance and dielectric loss

measurements were carried out at ambient temperature AC conductivity was calculated using equation 2 5 and dielectric constant by equation 2.8 as discussed in article 2.4.1 of Chapter 2.

5.4.5 (a) Conductivity versus frequency

Fig. 5.23(a) shows the variation of conductivity with frequency (freq. in Hz) for pristine and irradiated films. A sharp increase in conductivity has been observed in pristine as well as irradiated samples It is also observed that conductivity increases as fluence increases. The increase in conductivity due to irradiation may be attributed to scissioning of the polymer chains and resulting in an increase of the free radicals, unsaturation, etc. An AC field of sufficiently high frequency may cause a net polarization, which is out of the phase with the field. This results in increased AC conductivity, it appears at frequencies greater than that at which traps are filled or emptied [12-14].
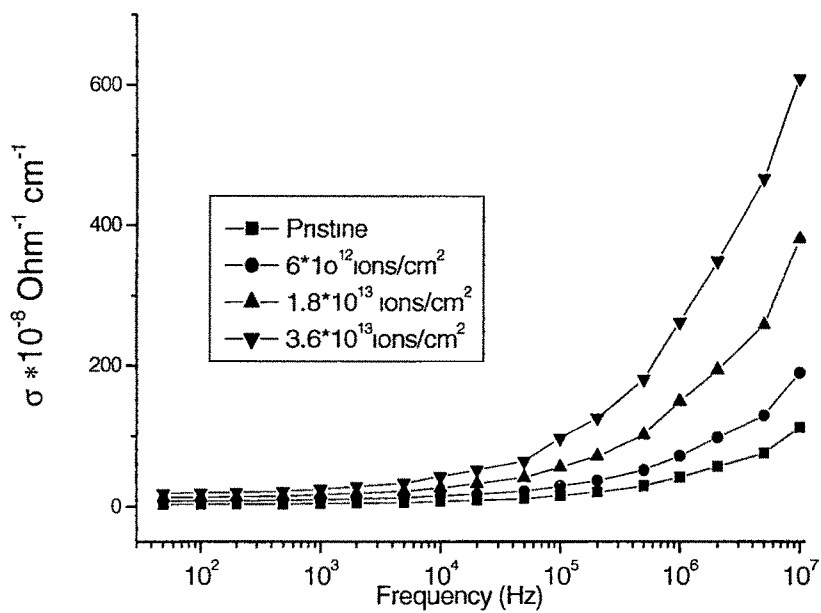
5.4.5 (b) tan δ versus frequency

Fig. 5.23(b) shows variation of dielectric loss (tan δ) with frequency for pristine and irradiated samples. It is observed that tan δ decreases sharply as frequency increases and become constant beyond a frequency of 1 kHz. It is also observed that dielectric loss (tan δ) increases as fluence increases. The increase in dielectric loss with fluence may be due to the scissioning of polymer chain and as a result increase in free radicals, unsaturation etc. The growth in tanδ as the increase in conductivity is brought about by an increase in the conduction of residual current and the conduction of of absorbance current [13], tanδ has positive values indicating the dominance of inductive behaviour.
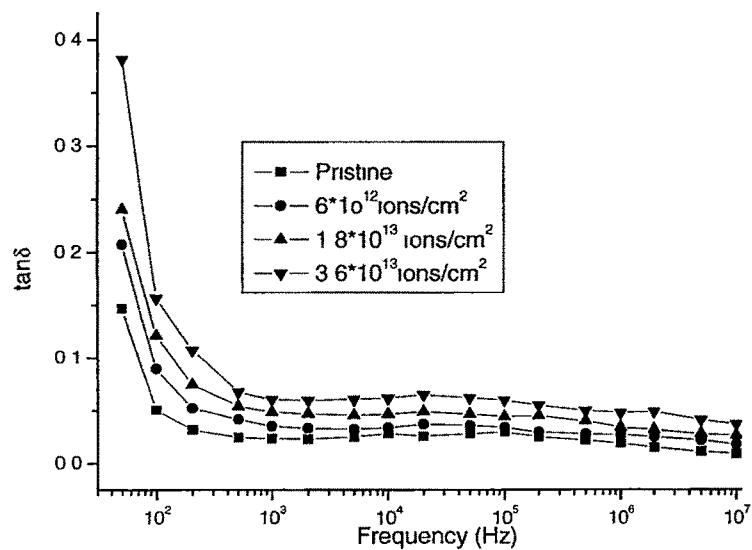
5.4.5 (c) Dielectric constant versus frequency

Fig. 5.23(c) shows the variation of dielectric constant with frequency for the pristine and irradiated samples. It is seen that the dielectric constant remains almost constant over a wide frequency range of 100 kHz and then decreases at higher frequencies. At lower frequencies, the mobility of the free charge carriers is constant and so dielectric constant remains unchanged. As frequency increases further (i.e. beyond 100 kHz), the charge carriers migrate through the dielectric and get trapped against a defect sites and induced an opposite charge in its vicinity. At these frequencies, the polarization of trapped and bound charges can not take place and hence the dielectric constant decreases [14]. It is also observed that dielectric constant increases as fluence increases. The increase in dielectric properties due to irradiation may be attributed to scissioning of polymer chains and as a result increase in free radicals and unsaturation etc. The dielectric constant decreases at higher frequencies (i.e. beyond 100kHz) obeys the Universal law of dielectric response given by $\varepsilon \propto f^{n-1}$, with n=0.43, n=0.45, n=0.46 and n= 0.47 for pristine and irradiated samples at the fluences of 6×10^{12}, 1.8×10^{13} and 3.6×10^{13} ions/cm^2 respectively. The observed nature of the fluence dependence of dielectric constant in studied frequency range can be explained by the prevailing influence of the enhanced free carriers due to the irradiation [14].
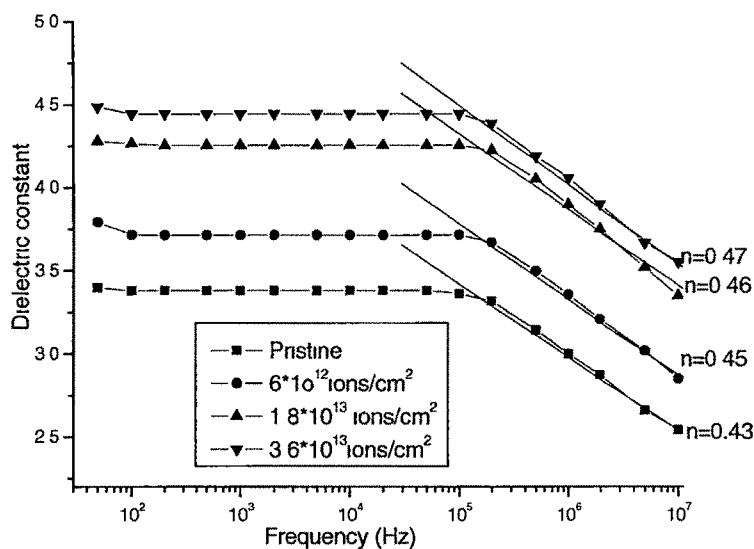
Figure 5.23(a) AC conductivity versus frequency for pristine and irradiated samples.

Figure 5.23(b) Dielectric loss versus frequency for pristine and irradiated samples.
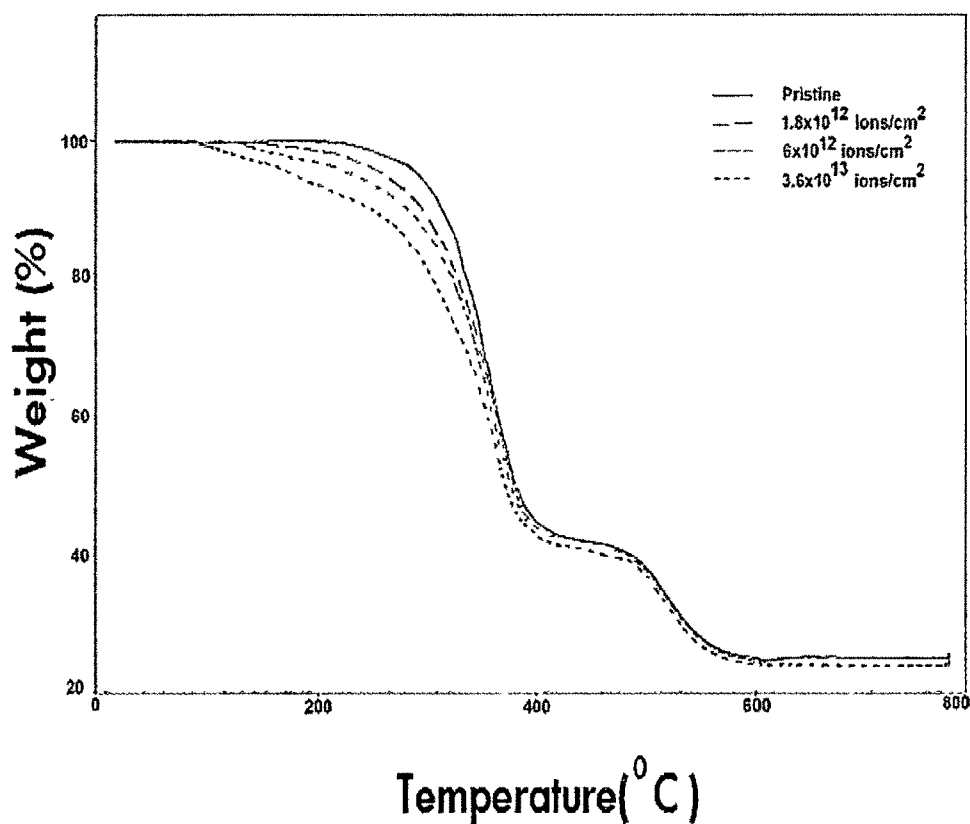
Figure 5.23(c) Dielectric constant versus frequency for pristine and irradiate samples.

5.4.6 Thermal Analysis

(Thermogravimetric Analysis and Differential Scanning Calorimetry)

The decomposition behavior of the polymer was examined by TGA as shown in Fig.5.24. The thermograms show two stages decomposition. TGA thermograms indicate a degradation of the polymer matrix under irradiation, making it to decompose earlier than the pristine sample. It is observed the thermal decomposition of the polymer depends upon the fluence of oxygen beam. As decipated in the figure, the stable zone for pristine sample is observed up to $190^{0}C$ and it decreases to $150^{0}C$, $130^{0}C$ & $100^{0}C$ at the fluences of $6x10^{12}$, $1.8x10^{13}$ and $3.6x10^{13}$ions/cm^2 respectively.The weight loss of pristine sample in the first stage of decomposition at 400^{0} C has been observed to 55%

and it increases to 57%, 58% and 59% as the fluence increases. No significant change has been observed at the second stage of decomposition for the pristine and irradiated samples.

Figure 5.24 TGA thermograms of pristine and irradiated samples.

The activation energy for the polymer decomposition process was calculated from the TGA patterns using the equation [31]

$$\ln[\ln(m_0/m)] = - E_a/R[1/T] + \text{constant}$$

Where E_a is the activation energy of decomposition, m_0 is the initial mass, m is the mass at temperature T and R is the universal gas constant. It is observed that activation energy (Fig. 5.25) decreases from 26.19 KJ/mole to 15.71 KJ/mole for pristine and irradiated

$(3.6 \times 10^{13}$ ions/cm$^2)$ samples. This indicates that irradiated sample decomposed earlier than pristine.
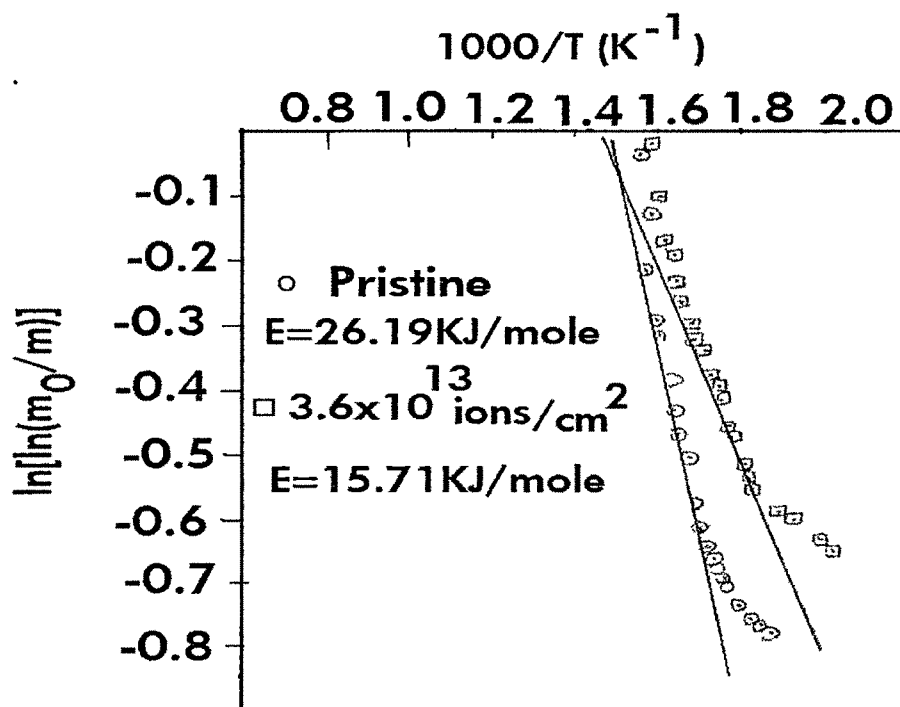

Figure 5.25 ln [ln(m$_0$/m)] versus 1000/T (K^{-1}) for the pristine and irradiated blend samples.

The DSC thermograms of pristine and irradiated samples are shown in Fig 5.26. The plot shows that there is no significant change in T$_g$ up to the fluence of 3.6×10^{13}ions/cm^2.
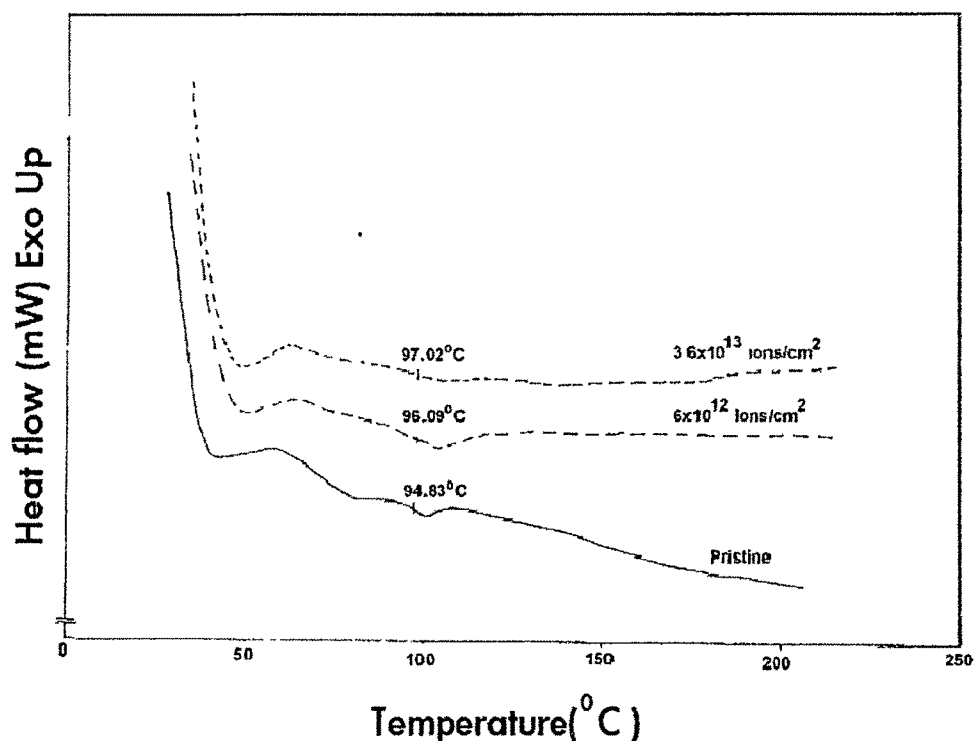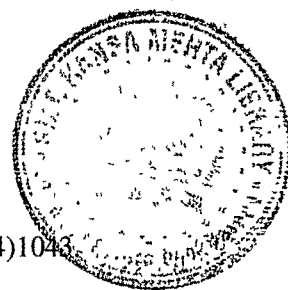
Figure 5.26 DSC thermograms of pristine and irradiated samples.

5.4.7 Conclusion

The AC electrical studies indicate that the conductivity increases on increasing the frequency and also with the fluence. Dielectric loss and constant are observed to change significantly with the fluence. This might be attributed to breakage of chemical bonds and resulted in the increase of free radicals, unsaturation etc. It is also observed that it obeys Universal law of dielectric response. The Vickers' hardness of the polymer increases as fluence increases, which can presumably due to the cross linking of some of the degraded molecules by irradiation i.e. formation of hydrogen depleted carbon network. The true bulk hardness of the film was obtained at loads greater than 400 mN. The calorimetric measurement of 80 MeV oxygen ions irradiated samples show no significant change in

219

glass transition temperature (T_g) TGA thermograms indicate that sample decomposed by losing hydrogen and other volatile constituents and convert polymeric structure into hydrogen depleted carbon network which makes polymer harder and more conducting.

References

[1]   E. H. Lee, G. R. Rao, M. B. Lewis, L. K. Mansur, J. Mater. Res. 9(1994)1043.

[2]   D.Xu, X.L. Xu, G.D.Du, R.Wang, S.C.Zou, and X.H.Liu, Nucl. Instr. & Meth. B
      80/81 (1993) 1063   .

[3]   D. Fink, F Hosci, H. Omichi, T. Sasuga, and L. Amaral, Rad. Eff. Def. in Solids,
      132, (1994) 313.

[4]   T. Terai and T. Kobayashi, Nucl. Instr. & Meth. B **166-167** (2000) 627.

[5]   H. S. Virk, P. S. Chandi and A. K. Srivastava, Bull. Mater. Sci. **24** (2001) 529.

[6]   R. Mishra, S. P. Tripathi, K. K. Dwivedi, D. T. Khathing, S. G. Ghosh, and D. Fink, Rad.
      Measure., **36**, (2003) 621.

[7]   N. Shah, N. L. Singh, C. F. Desai, and K. P. Singh, Rad. Measure. **36**, (2003) 699.

[8]   A. Sharma, N. L. Singh, M. S. Gadkari, V. Shrinet and D. K. Avasthi, J. Macromole. Sci.
      PAC **42** (2005) 149.

[9]   Anjum Qureshi, N. L. Singh, A. K. Rakshit, F. Singh, D.K.Avasthi, Surface and
      Coatings Technology in press (2007).

[10] J. P. Biersack, J. F. Ziegler, code SRIM-2003, The stopping range of ions in matter
      (IBM Research), New York, USA(2003).

[11] E.H.Lee,G.R.Rao and L.K.Mansur, Mat.Sci. Forum, **428-249** (1997) 135.

[12] A.K.Jonscher, Nature **267**(1997) 673.

[13] N. P. Bogoroditsky, V. V. Pasynkov, B. M. Tareev, Electrical engineering
      materials, Mir Publishers, Moscow (1974).

[14] A.K.Jonscher, Dielectric relaxation in solid, Chesla dielectric press, London, 1983.

221

[15] T Phukan, D Kanjilal, T D Goswami, H L. Das, Nucl. Instr and Meth. B 234(2005)520.

[16] C Jerome, S. Demoustier- Chnpagne, R Legras, R. Jerome, Chem. Eur J. 6(2000)3089.

[17] E Ferain, R. Legras, Nucl Instr. and Meth B 82 (1993)539.

[18] T Steckenreiter, E Balnzat, H.Fuess, C. Trautmann, Nucl. Inst. and Meth. B 151(1999) 161.

[19] MI Chipara, J. Reyes-Romero, Nucl Inst. and Meth. B 185 (2002)77.

[20] Z. Zhu, Y Sun, C Liu, J. Liu, Y. Jin, Nucl Inst. and Meth. B 193(2002) 271.

[21] Y.Wang, Y. Jin, Z. Zhu, C Liu, Y. Sun, Z. Wang, M. Hou, X. Chen, C. Zhang, J. Liu, B. Li, Nucl. Inst. and Meth. B 420(2000)164.

[22] F. Dehaye, E. Balanzat, E Ferain, R. Legras, Nucl. Instr. and Meth. B 209(2003)103.

[23] R. Mishra, S.P. Tripathy, K.K. Dwivedi, D.T. Khathing, S.Ghosh, D. Fink, Rad. Meas. 36(2003)719.

[24] N. L. Singh, Anjum Qureshi, F. Singh and D. K. Avasthi, Material Science and Engineering A 457(2007)195.

[25] E.H. Lee, Nucl Instr. and Meth. B151(1999)29.

[26] J. R. Woods, A.K.Pikaev, Applied Radiation Chemistry: Radiation Processing. John Wiley & Sons New York, USA, 1994.

[27] L.B.Bridwell, R.E.Giedd, Y.Q.Wang, S.S.Mohite, T.Jahnke, C.J.Brown, I.M.Bedell, and C.J.Sofield, Nucl.Instr. and Meth. B56-57 (1991)656.

[28] A.L.Evelyn,D.Ila, R.L. Zimmerman, K. Bhat, D.B Poker, D.K. Hensley, C.Klatt, S Kalbitzer, N. Just, C.Drevet, Nucl.Instr.and Meth. B148 (1999) 1141.

[29] R.Kumar, U.De, R.Prasad, Nucl. Instr. and Meth. B248(2006) 279.

[30] Anjum Qureshi, N.L.Singh, F Singh, D K Avasthi, Accepted for presentation in International conference on Materials for Advance Technologies,1-6 July, 2007, Singapore.

[31] A. Broido, J. Polym.Sci.7 (1969)1761

[32] S. K. Awasthi and W. R. Bajpai , Indian J Pure & Appl Phys 39 (2001) 795.

[33] N. L. Singh, A. Sharma, D. K Avasthi and. V Shrinet, Radiation effects in solids 160 (2005) 99.

[34] Y. S. Chaudhary, S. A. Khan, R. Shrivastav, V. R. Satsangi, S. Prakash, U. K. Tiwari , D. K. Avasthi, N.Gaswami and S. Dass, Thin solids films 492 (2005) 332 336.

[35] N.L.Singh, Anjum Qureshi, Sejal Shah, Dolly Singh, F.Singh, D.K.Avasthi, Presented in National Conference on Condensed Matter and Material Physics, 1- 3 Feb., 2007, Department, of Physics, Rajesthan University, Jaipur, India. To be published in Indian Journal of Pure and Applied Physics.

[36] A. Biswas, S. Lotha, D. Fink, J. P. Singh, D. K. Avasthi, B. K. Yadav, S K. Bose, D. T. Khathing, A. M. Avasthi, Nucl. Instr. And Meth. B 159 (1999) 40.